Simulating the Relaxation Dynamics of Microwave-Driven Zeolites

Aldo F. Combariza,[†] Ethan Sullivan,[†] Scott M. Auerbach,*[,†,‡] and Cristian Blanco[†,§]

Department of Chemistry and Department of Chemical Engineering, University of Massachusetts, Amherst, Massachusetts 01003, and Department of Chemistry, Universidad Industrial de Santander, AA 678 Bucaramanga, Colombia

Received: May 11, 2005; In Final Form: August 2, 2005

We have performed equilibrium and nonequilibrium molecular dynamics simulations to study how microwave (MW)-heated zeolite systems relax to thermal equilibrium. We have simulated the relaxation of both ionic and dipolar phases in FAU-type zeolites, finding biexponential relaxation in all cases studied. Fast-decay times were uniformly below 1 ps, while slow-decay times were found to be as long as 14 ps. Fast-decay times increase with an increase in the initial temperature difference between MW-heated ions/dipoles and the equilibrium system. Slow-decay times were found to be relatively insensitive to the details of the MW-heated nonequilibrium state. Velocity, force, and orientational correlation functions, calculated at equilibrium to explore the natural dynamics of energy transfer, decay well before 1 ps and show little evidence of biexponential decay. In contrast, kinetic energy correlation functions show strong biexponential behavior with slow-decay times as long as 14 ps. We suggest a two-step mechanism involving initial, efficient energy transfer mediated by strongly anharmonic zeolite−guest forces, followed by a slower process mediated by weakly anharmonic couplings among normal modes of the zeolite framework. In addition to elucidating relaxation from MW-heated states, we expect that these studies will shed light on energy transfer in other contexts, such as adsorption and reaction in zeolites, which often involve significant heat release.

I. Introduction

Zeolites are nanoporous, crystalline aluminosilicates with a rich variety of interesting properties and industrial applications.[1] The structural and chemical versatility offered by zeolites strongly suggests that other applications lie ahead for these materials. Over the past few years, a flurry of recent interest has emerged in studying adsorption,[2,3] ion exchange,[4] and reaction[5,6] in zeolites, as well as growth of zeolites[7−10] and other oxides,[11,12] all driven by microwave (MW) radiation.[13,14] Despite this significant research activity, there remains disagreement whether MW-driven zeolites really behave in ways that are qualitatively different from conventionally heated systems.[15,16] This disagreement is fueled in part by the lack of a fundamental, atomistic picture of energy transfer in such systems. In this article, we have applied equilibrium and nonequilibrium molecular dynamics (MD) to study how MW-heated zeolites relax to thermal equilibrium.

Over the last few decades, pioneering studies on energy transfer[17] and bond-selective chemistry[18] have found that intramolecular vibrational relaxation (IVR) typically occurs on subpicosecond time scales, making it difficult to exploit transient, nonstatistical energy distributions. This general notion has led many researchers to surmise that applying MW radiation to zeolites will yield an expensive form of conventional heating. In previous work, we have performed nonequilibrium MD simulations on MW-heated zeolites, finding a variety of circumstances under which athermal energy distributions can be produced.[19−21] Inspired by the IVR studies mentioned above, we applied MD in the present study to follow IVR of MW-heated zeolites. We find below that MW-heated zeolites require on the order of 10 ps for complete relaxation to equilibrium. This process is surprisingly slow compared to the conventional IVR discussed above.

Insights into the physical origin of this relatively slow relaxation can be sought from the fluctuation−dissipation theorem, which states that nonequilibrium disturbances decay in the same way as do correlations between spontaneous fluctuations at equilibrium.[22,23] Although the fluctuation−dissipation theorem is strictly only valid in the limit of small nonequilibrium disturbances, it provides useful insights for systems relatively far from equilibrium as well. For example, the fluctuation−dissipation theorem accurately describes equilibration (i.e., diffusion) from a step concentration profile.[24] Applying the fluctuation−dissipation theorem requires the identification of a microscopic quantity whose average is proportional to the macroscopic variable exhibiting relaxation. In the present case, the relevant microscopic quantity is the total kinetic energy of the ionic or dipolar phase adsorbed in a zeolite. We find below that the standard equilibrium correlation functions of velocity, force, and orientation bear little resemblance to relaxation of MW-heated zeolites. In contrast, we show that the kinetic energy correlation function captures both qualitative and quantitative aspects of relaxation of MW-heated zeolites.

We have simulated the relaxation of both ionic and dipolar phases in FAU-type zeolites, finding biexponential relaxation with slow-decay times as long as 14 ps. Kinetic energy correlation functions calculated at equilibrium show strong biexponential behavior with slow-decay times in good agreement with those obtained by relaxing MW-heated states. We suggest a two-step energy transfer mechanism mediated by zeolite−guest forces at short times and by zeolite framework anharmo-

* To whom correspondence should be addressed. E-mail: auerbach@chem.umass.edu.
[†] Department of Chemistry, University of Massachusetts.
[‡] Department of Chemical Engineering, University of Massachusetts.
[§] Department of Chemistry, Universidad Industrial de Santander.

10.1021/jp0524680 CCC: $30.25
Published on Web 09/08/2005

nicities at longer times. In addition to elucidating relaxation from MW-heated states, we expect that these studies will shed light on energy transfer in other contexts, such as adsorption and reaction in zeolites, which often involve significant heat release.

The remainder of this article is organized as follows: In section II, we outline the simulation methods used in the present study, in section III, we discuss the results of our equilibrium and nonequilibrium simulations, and in section IV, we offer concluding remarks.

II. Methods

In this section we describe various MD simulations performed on two FAU-type zeolites: NaY and siliceous FAU (Si−FAU).[25] We simulated a bare NaY zeolite, where the exchangeable Na ions are strong MW absorbers, and we studied methanol in Si−FAU, where methanol is expected to strongly absorb MW radiation. In what follows, we describe the models, potential surfaces, and MD simulations.

A. Zeolite Models. We have studied two different models of zeolites: NaY and Si−FAU. For the NaY system, we have chosen a Si:Al ratio of 2.0; this configuration corresponds to a unit cell containing 128 Si and 64 Al atoms, which requires 64 Na^+ ions to balance the charge.[26] The Al atoms are randomly distributed within the framework in accordance with Lowenstein's empirical rule, which forbids Al−O−Al linkages. The unit cell is completed by including 128 O_a atoms, which bridge Si and Al, and 256 O_s atoms to build Si−O−Si bridges. The cubic unit cell obtained has a lattice parameter of 24.7 Å[27] and a window aperture of about 7.5 Å. The Na^+ ions show high mobility when compared with framework atoms, thus allowing the Na^+ ions to be strongly excited by MW fields.

We have also simulated methanol adsorbed in Si−FAU zeolite, modeled with a single unit cell containing 192 Si atoms and 384 O_s atoms with a fixed lattice parameter of 24.3 Å.[26] The methanol loading was set to 32 molecules per unit cell (4 molecules per supercage). This relatively high loading ensures sufficient statistics in the relaxation and correlation simulations discussed below. For both zeolite systems, short-range interactions were cutoff at 12.0 Å. Standard periodic boundary conditions were implemented via the minimum image convention and Ewald summations.[28]

B. Potential Energy Surface. The potential energy function used in the present simulations was reported previously by us in ref 20. We refer the reader to this article for details on the potential function and its parameters. In general, the function has the form

$$V = V_Z + V_M + V_{ZM} + V_{MM} \tag{1}$$

where V_Z controls zeolite vibrations, V_M controls methanol intramolecular vibrations, and V_{ZM} and V_{MM} are the zeolite−methanol and methanol−methanol intermolecular interactions, respectively. Electrostatic contributions to V_Z, V_{ZM}, and V_{MM} are calculated using fixed point charges and Ewald summations. Short-ranged contributions to V_Z are modeled with the Buckingham (exp-6) form, and for V_{ZM} and V_{MM} we used the Lennard-Jones (12−6) form. For V_M, we used our valence bond form reported in ref 20.

C. Molecular Dynamics Simulations. We have used our program DIZZY[29] to perform two different types of MD simulations: nonequilibrium molecular dynamics (NEMD) and equilibrium molecular dynamics (EMD). The NEMD simulations were performed to produce MW-driven steady states as initial conditions to follow relaxation to equilibrium. The EMD simulations were performed to follow the dynamics of equilibration and to calculate equilibrium correlation functions in an effort to elucidate the time scales of relaxation dynamics.

MW-driven steady states were simulated via NEMD by applying an external MW field according to[19−21]

$$\frac{d\vec{r}_i}{dt} = \frac{\vec{p}_i}{m_i} \qquad \frac{d\vec{p}_i}{dt} = -\frac{\partial V}{\partial \vec{r}_i} + q_i\vec{E}_t \tag{2}$$

where $\vec{r}_i$ and $\vec{p}_i$ are the three-dimensional (3D) position and momentum of particle i, respectively, m_i and q_i are its mass and charge, and $V = V(\vec{r}_1,\vec{r}_2, ...,\vec{r}_N)$ is the zeolite + guest potential energy function described above. All zeolite and guest atoms are allowed to move in our simulations. The additional electrostatic force in eq 2, namely, $q_i\vec{E}_t$, attempts to push charged particles to the left or right along the z-axis, depending upon the sign of the charge and the phase of the electric field. Such forces can excite vibrations of zeolite atoms and can excite external vibrations and librations of guest molecules in zeolites.

Steady states were obtained from MW-driven systems using the Andersen thermostat,[30] which replaces the 3D velocities of randomly selected atoms at random times with those extracted from Maxwell−Boltzmann distributions, as discussed in our previous work.[19−21] All zeolite and guest atoms are subjected to random velocity replacement at random times. The Andersen thermostat has been implemented by specifying three parameters: the target temperature, the number of atoms to be replaced at a time, and the average time between replacements. Target temperatures for the simulations below were set to 200 and 300 K for both zeolite systems. Actual steady-state temperatures exceed a given target temperature because of MW heating.

The MW field intensity was chosen to be suffiently high to observe a significant response in a reasonable time scale. The field strengths we used were 0.3 and 1.8 V/Å for NaY and for methanol in Si−FAU, respectively, both with a frequency of $\nu = 1.5 \times 10^{11}$ Hz. The systems were equilibrated for 5 ps before applying the MW field and the thermostat. After turning on the external field and thermostat, we evolved the systems for 100 ps to reach robust steady states.

Thermal relaxation simulations of NaY and methanol in Si−FAU were performed by monitoring subsystem temperatures as a function of time. For NaY, we monitored the overall temperature of Na cations (T_{Na}) and that of the NaY system (T_{NaY}). For methanol in Si−FAU, we tracked the overall center-of-mass temperature of adsorbed methanols (T_{Me}) and that of the whole system ($T_{FAU-Meth}$). Initial conditions for thermal relaxation simulations were extracted from MW-driven steady states. Thermal relaxation simulations were performed by running MD without the MW field and without the Andersen thermostat. As such, relaxation simulations are simply NVE MD simulations started from MW-heated initial conditions. We omitted the thermostat because our simulations include the dynamics of zeolite frameworks, which act as effective heat baths at equilibrium. Including a thermostat during relaxation is thus unnecessary and, further, can artificially influence the kinetics of thermalization.

Subsystem temperature profiles from individual relaxation simulations were found to exhibit significant noise. To generate statistically significant relaxation signals, 100 identical runs were averaged from initial conditions extracted from steady states. We found that recognizable relaxation signals could only be obtained by averaging over MD runs initiated from time points corresponding to nodes of the MW field. This phase locking could likely be avoided by considering much larger system sizes,

allowing averages over many more Na cations or methanol molecules. However, such simulations are computationally prohibitive and are likely unnecessary. This is because phase-locked averages involve negligible molecular correlations since the time period of our MW field is relatively long (ca. 6.7 ps). Relaxation signals so obtained were fitted to single-exponential and double-exponential decay functions. In general, we found that single-exponential fits were unacceptable, while double-exponential functions fitted the relaxation data quite accurately.

Inspired by the fluctuation−dissipation theorem,[23] we performed EMD on NaY and on methanol/Si−FAU to calculate equilibrium correlation functions in an effort to elucidate the natural relaxation dynamics of these systems. For Na^+ in NaY, we calculated velocity and zeolite−guest force autocorrelation functions. For methanol in Si−FAU, we calculated velocity and zeolite−guest force autocorrelation functions for methanol's center-of-mass, as well as the orientational correlation function of methanol's C−O bond axis. In general, we found that all these correlation functions decay much too rapidly to account for the relaxation kinetics reported below. Also, these correlation functions showed little evidence of biexponential behavior. We then calculated kinetic energy autocorrelation functions for Na and for methanol's center-of-mass, because kinetic energy is the microscopic variable corresponding to the subsystem temperature considered in relaxation simulations. All these equilibrium correlation functions were computed in the standard fashion,[28] averaging dynamics from single, long EMD runs lasting longer than 1.0 ns. We attempted to fit the resulting kinetic energy correlation functions to single-exponential and double-exponential functions. As with the relaxation signals, single-exponential fits were found to be unsatisfactory, while double-exponential fits showed good accuracy. Time scales from relaxation simulations and kinetic energy autocorrelation functions are discussed below.

III. Results and Discussion

Here we present results of MW-driven MD simulations of NaY zeolite and methanol in Si−FAU zeolite, both under athermal steady-state conditions. Next we present the results of relaxation simulations, probing the equilibration dynamics of MW-heated athermal states of NaY and methanol/Si−FAU. Finally, we discuss several equilibrium correlation functions of these zeolite systems to eluciate the natural dynamics of equilibration.

A. Microwave-Driven Steady States. Steady-state temperature profiles for NaY and methanol/Si−FAU are shown in Figure 1. When thermostating at 200 K, MW-heated NaY reaches a steady-state temperature of 220 K, while thermostating at 300 K yields a MW-heated steady state at 338 K. In both cases, the steady states exhibit robust dynamical stability for well over the 1.5 ns shown in Figure 1. These two steady states were produced to explore whether equilibration time scales depend on details of the initially prepared nonequilibrium states. We explored the same question for methanol/Si−FAU by producing two different steady states for that system. When thermostating at 200 and 300 K, MW-heated methanol/Si−FAU reaches steady-state temperatures of 351 and 449 K, respectively. Steady states of methanol/Si−FAU also show robust dynamical stability.

B. Relaxation to Equilibrium. The temperatures in Figure 1 reflect the total kinetic energies in each system. These quantities do not reveal the fact that Na is relatively hot in MW-heated NaY and that methanol is relatively hot when MW-heated in Si−FAU.[20] To follow the equilibration of these systems, we

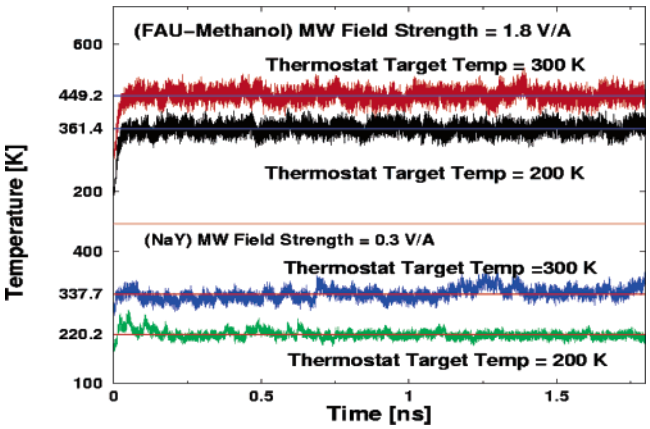

Figure 1. Steady states for methanol/Si−FAU and for NaY at thermostat temperatures 200 and 300 K. MW field strengths are 1.8 V/Å for methanol in Si−FAU and 0.3 V/Å for NaY. Average steady-state temperatures are shown.

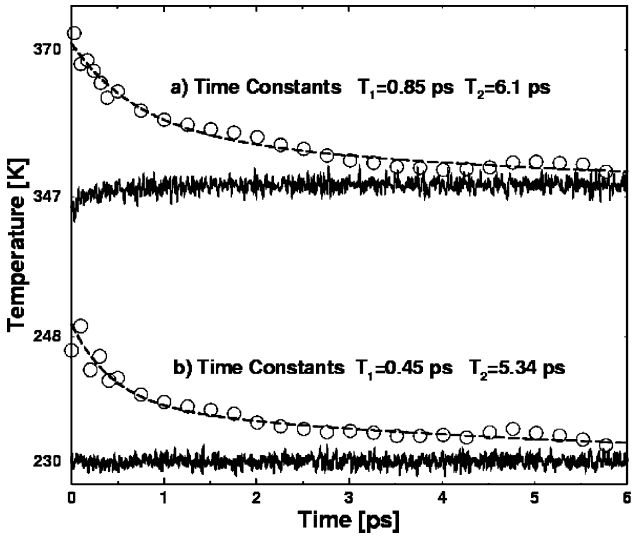

Figure 2. Thermal relaxation of Na in NaY from two different MW-heated steady states. Bottom relaxation is from the steady state using 200 K thermostat target temperature; top relaxation is from the 300 K target temperature. Circles/lines are Na/Y-framework temperatures from MD; dashed lines are biexponential fits to Na temperatures.

computed subsystem temperatures T_{Na} for Na in NaY, and T_{Meth} for methanol in Si−FAU, shown in Figures 2 and 3, respectively. In general, these relaxation curves are found to exhibit biexponential decay; this is most obvious in the top of Figure 3.

The Na temperature T_{Na} relaxes from 248 K to a final equilibrium value of 230 K (Figure 2) starting from the NaY steady state at 220 K (Figure 1). (We note that the system equilibrates to a temperature (230 K) higher than the steady-state temperature (220 K) because the MW-heated potential energy has a higher effective temperature than that of the kinetic energy, as shown in our previous work.[21]) The two time scales extracted from the biexponential fit to this relaxation process are 0.45 and 5.34 ps. The NaY steady state at 338 K gives Na relaxation from 370 to 347 K, with time scales 0.85 and 6.10 ps. Here we observe a weak trend toward increasing relaxation times with an increase in the initial temperature difference between Na and the equilibrium system. We also find that the shorter time scale appears more sensitive to the details of the steady state, almost doubling from the lower temperature relaxation to the higher temperature one. In contrast, the longer time scale increases by only 14%.

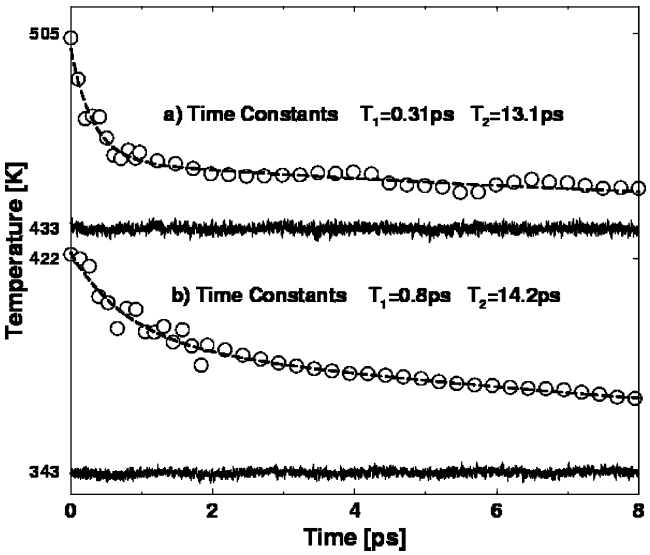

Figure 3. Thermal relaxation of methanol in Si−FAU from two different MW-heated steady states. Bottom relaxation is from the steady state using 200 K thermostat target temperature; top relaxation is from the 300 K target temperature. Circles/lines are methanol/Si−FAU temperatures from MD; dashed lines are biexponential fits to methanol temperatures.

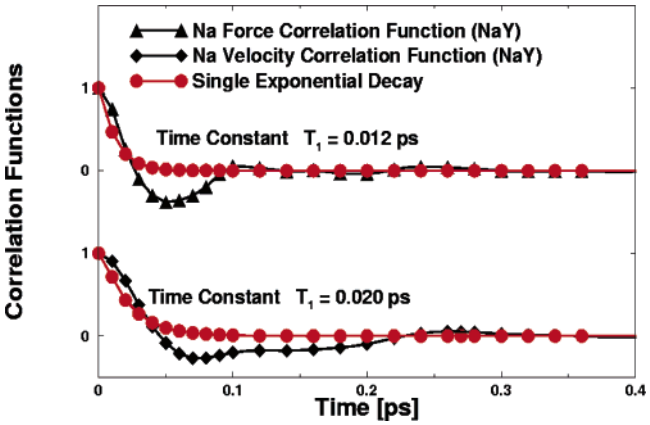

Figure 4. Equilibrium force and velocity correlation functions for Na in NaY.

Methanol cools from 422 to 343 K (79 K drop) with time scales 0.80 and 14.2 ps (Figure 3) starting from the methanol/Si−FAU steady state at 351 K (Figure 1). Methanol in the 449 K steady state cools from 505 to 433 K (72 K drop) with time scales 0.31 and 13.1 ps. For methanol in Si−FAU, we see a weak trend toward increasing relaxation times with an increase in the initial temperature difference between methanol and the equilibrium system, as was found above for Na in NaY. We also observe for methanol/Si−FAU that the shorter time scale appears more sensitive to the details of the steady state, as was found above for Na in NaY.

In general, the slow-decay times, 5−6 ps for NaY and 13−14 ps for methanol/Si−FAU, are surprisingly long time scales for thermal relaxation. Below we discuss possible mechanisms explaining these equilibration dynamics.

C. Equilibrium Correlation Functions. We calculated several equilibrium correlation functions to explore whether the relatively slow biexponential decay, found during relaxation to equilibrium, can be found at equilibrium as well. Figure 4 shows velocity and force autocorrelation functions for Na in NaY. These functions decay well before 1 ps and show little evidence of biexponential decay. Figure 5 shows the same correlation

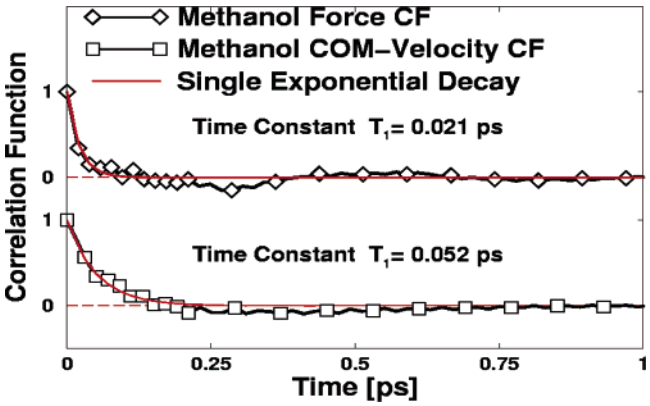

Figure 5. Equilibrium force and velocity correlation functions for methanol center-of-mass in Si−FAU.

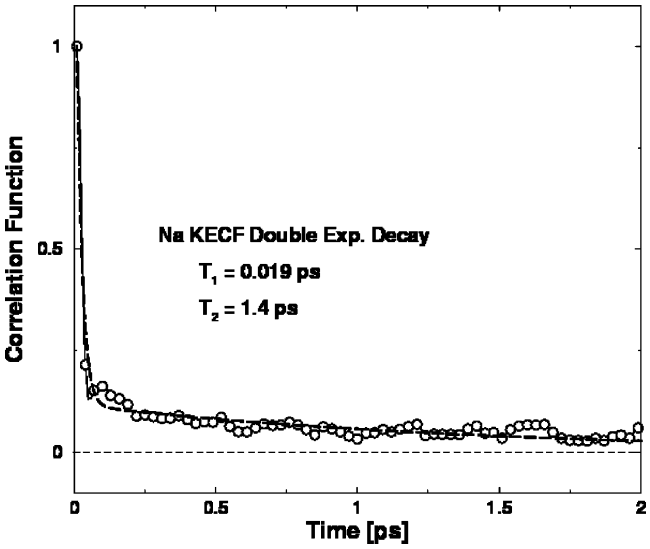

Figure 6. Equilibrium kinetic energy correlation function (circles) and biexponential fit (dashed line) for Na in NaY zeolite.

functions for the center-of-mass of methanol at equilibrium in Si−FAU. These functions likewise decay well before 1 ps with little evidence of biexponential decay. We thus find no evidence for the relatively slow biexponential behavior in these equilibrium correlation functions.

Some insight into this can be gleaned from the fluctuation−dissipation theorem, which states that nonequilibrium disturbances decay in the same way as do correlations between spontaneous fluctuations at equilibrium.[22,23] Applying the fluctuation−dissipation theorem requires the identification of a microscopic quantity whose average is proportional to the macroscopic quantity exhibiting nonequilibrium relaxation. The microscopic quantity that corresponds to T_{Na} is the total kinetic energy of Na atoms in NaY and that for T_{Meth} is the total kinetic energy of methanols in Si−FAU. These ideas can be expressed mathematically according to

$$\frac{\Delta\bar{T}(t)}{\Delta\bar{T}(0)} = \frac{\langle \delta K(0)\delta K(t)\rangle}{\langle \delta K(0)\delta K(0)\rangle} \qquad (3)$$

Figure 6 shows the kinetic energy autocorrelation function for Na at equilibrium in NaY at 300 K. This function shows clear biexponential decay, with a slow-decay time of 1.4 ps. Figure 7 shows the same correlation function for methanol in Si−FAU at 300 K, also showing clear biexponential behavior with a slow-decay time of 9.2 ps. Tables 1 and 2 summarize the relaxation times and kinetic energy correlation function decay times for

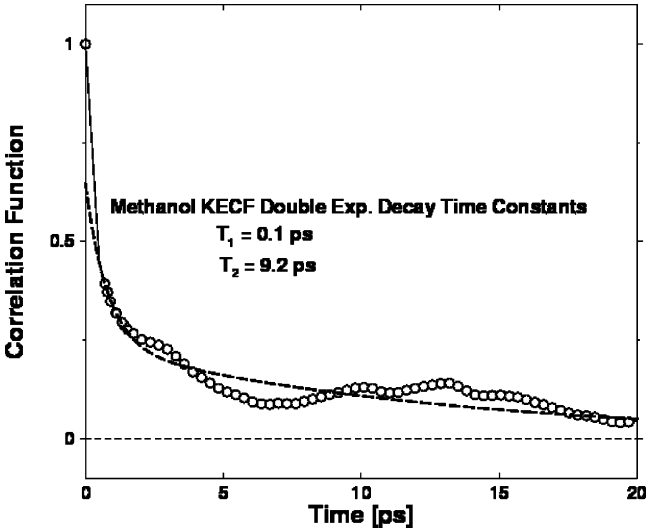

Figure 7. Equilibrium kinetic energy correlation function (circles) and biexponential fit (dashed line) for methanol in Si−FAU zeolite.

TABLE 1: Biexponential Decay Times for Na in NaY Zeolite

thermostat temp (K)	relaxation of Na from MW steady states		Na kinetic energy correlation function	
	τ_1 (ps)	τ_2 (ps)	τ_1 (ps)	τ_2 (ps)
200	0.45	5.34	0.017	1.24
300	0.85	6.1	0.019	1.4

TABLE 2: Biexponential Decay Times for Methanol in Si−FAU Zeolite

thermostat temp (K)	relaxation of MeOH from MW steady states		MeOH kinetic energy correlation function	
	τ_1 (ps)	τ_2 (ps)	τ_1 (ps)	τ_2 (ps)
200	0.81	14.2	0.12	13.6
300	0.31	13.1	0.10	9.2

NaY and methanol/Si−FAU, respectively. These show quite broad agreement, especially between the slow-decay times for methanol in Si−FAU as obtained from relaxation and equilibrium calculations.

The fact that the decay of the kinetic energy correlation function resembles that of the temperature relaxation simulations is encouraging, but it does not make the mechanism of energy transfer readily obvious. A clue may be found in the fact that the kinetic energy correlation function is a collective property of the entire guest phase, whereas the velocity and force correlation functions shown in Figures 4 and 5 probe only local dynamics. This leads us to the following hypothetical two-step mechanism of energy transfer.

Step one involves a MW-excited ion or dipole losing energy through collisions with nearby atoms of the zeolite, causing local framework heating. This process is mediated by zeolite−guest forces, which are relatively anharmonic and hence lead to rapid energy transfer. This continues until the ion or dipole and the local patch of zeolite have reached a quasi-equilibrium. Further energy transfer (and hence equilibration) relies on this locally hot patch of zeolite exchanging energy with the rest of the framework, which is step two. This step requires energy transfer among collective vibrations of the zeolite, which is mediated by forces that are nearly harmonic[31−35] and hence lead to much slower relaxation than in step one. Thus, we hypothesize that the biexponential relaxation reflects two energy transfer mechanisms with vastly different efficiencies: one mediated by strongly anharmonic zeolite−guest forces and the other mediated by weakly anharmonic couplings among normal modes of the zeolite framework. This hypothesis will be tested in a forthcoming publication.

IV. Concluding Remarks

We have performed equilibrium and nonequilibrium molecular dynamics simulations to study how MW-heated zeolite systems relax to thermal equilibrium. We have simulated the relaxation of both ionic and dipolar phases in FAU-type zeolites, finding biexponential relaxation in all cases studied. Fast-decay times are uniformly below 1 ps, while slow-decay times can be as long as 14 ps. Fast-decay times increase with an increase in the initial temperature difference between MW-heated ions/dipoles and the equilibrium system. Slow-decay times are relatively insensitive to the details of the MW-heated nonequilibrium state. Velocity, force, and orientational correlation functions, calculated at equilibrium to explore the natural dynamics of energy transfer, decay well before 1 ps and show little evidence of biexponential decay. In contrast, kinetic energy correlation functions show strong biexponential behavior with slow-decay times as long as 14 ps. We suggest a two-step mechanism of energy transfer involving initial, efficient energy transfer mediated by strongly anharmonic zeolite−guest forces and followed by a slower process mediated by weakly anharmonic couplings among normal modes of the zeolite framework.

These simulations provide atomistic insights into the relaxation of MW-heated systems. This should help experimentalists determine when to expect MW-heated zeolites to exhibit novel athermal phenomena on microscopic length and time scales. In addition, the subject of energy transfer in zeolites goes beyond MW-heating experiments. For example, adsorption and reaction in zeolites often involve significant heat release. Our finding of biexponential relaxation mediated by zeolite−guest and zeolite−zeolite forces may elucidate energy transfer during adsorption and reaction in zeolites as well.

Acknowledgment. We acknowledge generous funding from the National Science Foundation Nanoscale Interdisciplinary Research Team program (NSF CTS-0304217) and from the UMass Amherst Department of Chemistry for computational resources.

References and Notes

(1) Auerbach, S. M., Carrado, K. A., Dutta, P. K., Eds. *Handbook of Zeolite Science and Technology*; Marcel Dekker: New York, 2003.
(2) Kobayashi, S.; Kim, Y.-K.; Kenmizaki, C.; Kushiyama, S.; Mizuno, K. *Chem. Lett.* **1996**, *9*, 769−770.
(3) Turner, M. D.; Laurence, R. L.; Conner, W. C.; Yngvesson, K. S. *AIChE J.* **2000**, *46*, 758−768.
(4) Lopes, J. M.; Serralha, F. N.; Costa, C.; Lemos, F.; Ribeiro, R. R. *Catal. Lett.* **1998**, *53*, 103−106.
(5) Hajek, M. *Collect. Czech. Chem. Commun.* **1996**, *62*, 347−354.
(6) Marun, C.; Conde, L. D.; Suib, S. L. *J. Phys. Chem. A* **1999**, *103*, 4332−4340.
(7) Mintova, S.; Mo, S.; Bein, T. *Chem. Mater.* **1998**, *10*, 4030−4036.
(8) Cundy, C. S. *Collect. Czech. Chem. Commun.* **1998**, *63*, 1699−1723.
(9) Rao, K. J.; Vaidhyanathan, B.; Ganguli, M.; Ramakrishnan, P. A. *Chem. Mater.* **1999**, *11*, 882−895.
(10) Conner, W. C.; Tompsett, G.; Lee, K.; Yngvesson, K. S. *J. Phys. Chem. B* **2004**, *108*, 13913−13920.
(11) Peelamedu, R. D.; Roy, R.; Agrawal, D. K. *J. Mater. Res.* **2001**, *344* (10), 2770−2772.
(12) Peelamedu, R. D.; Roy, R.; Agrawal, D. *Mater. Res. Bull.* **2001**, *36*, 2723−2739.
(13) Ayappa, K. G. *Rev. Chem. Eng.* **1997**, *13* (2), 1.
(14) Pozar, D. M. *Microwave Engineering*, 2nd ed.; John Wiley & Sons: New York, 1998.
(15) Stuerga, D. A. C.; Gaillard, P. *J. Microwave Power Electromagn. Energy* **1996**, *31*, 87−100.

(16) Stuerga, D. A. C.; Gaillard, P. *J. Microwave Power Electromagn. Energy* **1996**, *31*, 101−113.
(17) Levine, R. D.; Bernstein, R. B. *Molecular Reaction Dynamics and Chemical Reactivity*; Oxford University Press: New York, 1987.
(18) Metz, R. B.; Thoemke, J. D.; Pfeiffer, J. M.; Crim, F. F. *J. Chem. Phys.* **1993**, *99*, 1744−1751.
(19) Blanco, C.; Auerbach, S. M. *J. Am. Chem. Soc.* **2002**, *124*, 6250−6251.
(20) Blanco, C.; Auerbach, S. M. *J. Phys. Chem. B* **2003**, *107*, 2490−2499.
(21) Blanco, C.; Auerbach, S. M. *J. Comput. Theor. Nanosci.* **2003**, *1*, 180−186.
(22) Onsager, L. *Phys. Rev.* **1931**, *37*, 405.
(23) Chandler, D. *Introduction to Modern Statistical Mechanics*; Oxford University Press: New York, 1987.
(24) Maginn, E. J.; Bell, A. T.; Theodorou, D. N. *J. Phys. Chem.* **1993**, *97*, 4173−4181.
(25) Baerlocher, C.; Meier, W. M.; Olson, D. H. *Atlas of Zeolite Framework Types*, 5th ed; Elsevier: Amsterdam, The Netherlands, 2001.
(26) Hriljac, J. A.; Eddy, M. M.; Cheetham, A. K.; Donohue, J. A.; Ray, G. J. *J. Solid State Chem.* **1993**, *106*, 66−72.
(27) Fitch, A. N.; Jobic, H.; Renouprez, A. *J. Phys. Chem.* **1986**, *90*, 1311.
(28) Frenkel, D.; Smit, B. *Understanding Molecular Simulations*; Academic Press: San Diego, CA, 1996.
(29) Henson, N. J. Ph.D. Thesis, Oxford University, 1996.
(30) Andersen, H. C. *J. Chem. Phys.* **1980**, *72*, 2384−2393.
(31) Kong, Y. S.; Jhon, M. S.; No, K. T. *Bull. Korean Chem. Soc.* **1985**, *6*, 57−60.
(32) Iyer, K. A.; Singer, S. J. *J. Phys. Chem.* **1994**, *98*, 12679−12686.
(33) Kopelevich, D. I.; Chang, H. C. *J. Chem. Phys.* **2001**, *114*, 3776−3789.
(34) Turaga, S. C.; Auerbach, S. M. *J. Chem. Phys.* **2003**, *118*, 6512−6517.
(35) Astala, R.; Auerbach, S. M.; Monson, P. A. *Phys. Rev. B* **2005**, *71*, 014112.